Journal of Materials Science and Engineering A 10 (5-6) (2020) 81-88
doi: 10.17265/2161-6213/2020.5-6.001

Effect of Titanium on the Martensitic Transformation Temperature of Cu-14Al-4Ni Shape Memory Alloy Rapidly Solidified

Nicole Araujo[1], Marília Bortolotto[1], Marlon Silva[1], Marcelo Nava[2], Pedro Lima[1] and Emmanuel Lima[3]

1. DATM, Federal Institute of Education, Science and Technology of Bahia (IFBA), Salvador-BA, 40301-015, Brazil

2. Federal Institute of Education, Science and Technology of Bahia–IFBA, Barreiras-BA, 47808-006, Brazil

3. Faculdade do Gama (FGA), Universityof Brasília (UnB), Gama-DF, 72444-240, Brazil

Abstract: The present research aimed to analyze the influence that different contents of titanium (x = 0.5, 0.6 and 0.7 wt.%) have on the martensitic transformation temperature of a Cu-14Al-4Ni (wt.%) SMA (shape memory alloy). The Cu-14Al-4Ni-xTi samples were casted in an arc-melting furnace and rapidly solidified. All samples underwent heat treatment in a tubular furnace at a temperature of 1,100 °C for 30 min and water quenched at 25 °C. Subsequently, samples were analyzed by SEM (scanning electron microscopy) with EDS (energy dispersive spectroscopy), XRD (X-ray diffraction) and DSC (differential scanning calorimeter). SEM images and XRD patterns showed that the presence of titanium modified the alloy's microstructure, induced the formation of three titanium rich phases called "X" phase ($CuNi_2Ti$, Cu_3Ti and $AlCu_2Ti$) and reduced the presence of the brittle phase γ_2 (Cu_9Al_4) for samples with 0.6 and 0.7 wt.% Ti. The titanium added to the copper based SMA also functioned as a refiner, reducing GS (grain size) up to approximately 80% with the increase of Ti content. DSC results exhibited low enthalpy levels, hysteresis, as well as low start martensitic transformation temperatures.

Key words: Cu-14Al-4Ni, titanium, SMA, martensitic transformation temperature, "X" phase.

Nomenclature

SMA	shape memory alloy
SME	shape memory effect
SEM	scanning electron microscopy
EDS	energy dispersive spectroscopy
XRD	X-ray diffraction
DSC	differential scanning calorimeter
RMT	reversible martensitic transformations
CT	critical temperatures

Greek Letters

2θ	diffraction angle
β'_1	martensitic phase
γ_2	brittle phase

1. Introduction

The SMAs' (shape memory alloys) properties are mostly related to the reversible martensitic transformations (RMT) that usually occur in a temperature range of -100 °C to 300 °C, depending on the alloy's composition. The RMTs are characterized by low energy and elevated interface mobility between phases, martensitic and matrix, when subjected to small temperatures variations or strain application. These characteristics, associated to symmetry alteration during the transformations result in crystallographic reversible thermoelastic martensitic transformations [1].

There are many alloys that exhibit SME (shape memory effect) such as Ni-Ti, copper and iron-based alloys [2]. The copper based SMAs have been attracting attention of scientists and researches due to low cost, wide range of transformation temperature, high thermal stability and low hysteresis level, as well as their easy production. Among them, the Cu-14Al-4Ni (wt.%) offers a greater potential for

Corresponding author: Pedro Lima, Ph.D., professor, researchfields: materials science, mechanical engineering.

engineering applications because of its high transformation temperatures [3] and better thermal stability comparing to the Cu-Zn-Al. However, due to its susceptibility to brittle intergranular fracture, caused by elastic anisotropy, multiple nucleation of cracks on the grain boundaries occur, which limits its industrial application. Nonetheless, the low ductility of the Cu-14Al-4Ni polycrystalline alloy can be enhanced by grain refinement through the addition of Ti, Nb, B, Mn, for instance [4].

The rapid solidification process can form structures with very particular characteristics and of great technological interest, such as: grain refinement, homogeneous structure without segregation, supersaturated solid solutions, metastable phases and amorphous structures [5]. These structures can mitigate the effects that cause SME degradation.

Nevertheless, it is necessary research regarding the influence of refining elements addition on thermal behavior for Cu-14Al-Ni SMAs, associated with an adequate obtaining method. Therefore, low cost would not be the only criteria for selection, but also the alloys peculiar properties can be explored more efficiently and emphasizing less on the alloys degradation.

In this study, different contents of titanium were added to a Cu-14Al-4Ni by arc-melting and rapid solidification process. The main objective was to relate phase transformation temperatures and thermal enthalpy levels, with phases formed and GS (grain size).

2. Methodology

The elements selected to produce the alloy had a high purity level (99.99%). Cu-14Al-4Ni (wt.%) and *x* Ti (*x* = 0.5, 0.6 and 0.7 wt.%) were casted in a arc-melting furnace, in an inert atmosphere with argon gas, and solidified rapidly in a copper mold at a temperature of 20 °C. There were obtained four ingots with a flat shape (3 mm × 5 mm × 35 mm) of approximately 5 g each.

Temperature and time of heat treatment (betatization) were extracted from a thermal analysis. Each alloy underwent a heating of 30 °C up to 1,400 °C in a 50 °C/min rate in Calorimeter SDQ600 TA Instruments of Differential Thermal Analysis. After the analysis results, all samples were heat treated in a tubular furnace with argon gas, at 1,100 °C, for 30 min and water quenched at 25 °C.

Micro-structural and properties characterization were performed with SEM (scanning electron microscopy), EDS (energy dispersive spectroscopy), XRD (X-ray diffraction) and DSC (differential scanning calorimeter). SEM (TESCAN model LMU VEGA 3) was used to evaluate the martensitic evolution and new phases formed by adding titanium. Along with SEM, EDS mapping was applied to verify chemical composition in 5 different sample zones. XRD analyses were carried out in a Shimadzu model XRD-7000, radiation CuKα, with 2θ ranging between 20° and 100°, and a 1°/min scanning step. In order to identify and quantify the formed phases, Rietveld method was used with softwares Maud and X-pert HighScore. DSC analyses were executed in Perkin Elmer DSC8000, with a 10°/min rate varying the temperature from 0 °C to 250 °C. The calculation of GS was done through first direct measurement with SEM, based on ASTM E112, and use of Eq. (1) [6], where G is the ASTM grain size and L is the measured grain length, in millimeters.

$$G = - 3{,}2877 – [6{,}6439 \times \log (Lmm)] \quad (1)$$

3. Results and Discussion

3.1 Material Composition

The alloys' chemical composition, determined by EDS mapping, is shown in Table 1. The compositions mapped are in agreement with the nominal percentages attributed to the obtained alloys. This is supported by the information that a vacuum process and rapid solidification contribute to the material chemical composite control [7, 8].

Table 1 Samples chemical composition analyzed by EDS (wt.%)

Alloys	Cu	Al	Ni	Ti
0.0%Ti	81.08 ± 0.09	15.26 ± 0.04	3.66 ± 0.05	0.00
0.5%Ti	81.60 ± 0.07	14.70 ± 0.04	3.70 ± 0.06	0.56 ± 0.02
0.6%Ti	82.86 ± 0.04	13.43 ± 0.03	3.71 ± 0.04	0.58 ± 0.01
0.7%Ti	80.91 ± 0.10	14.64 ± 0.04	3.78 ± 0.06	0.67 ± 0.02

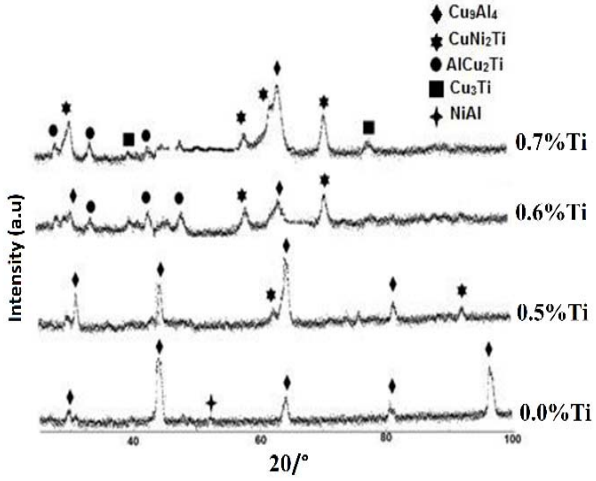

Fig. 1 XRD patterns for all samples after heat treatment.

3.2 XRD Patterns

Fig. 1 shows the crystalline structure evolution of the studied alloys after heat treatment and quenching [9]. The CuAlNi alloy exhibited predominant phase (Cu_9Al_4), caused by the decomposition of phase, of polycrystalline characteristics, which tends to increase the alloy brittleness [9]. XRD analysis showed a microstructure with phase (90.7%) and presence of phase (9.3%), of chemical formula NiAl. The phase exhibits a typical martensitic structure (β'_1 30.19° and 63.5°).

The 0.5%Ti presented 4.98% of "X" phase, of chemical composition $CuNi_2Ti$ and γ_2 phase (95.02%). However, for 0.6%Ti, the addition of 0.6% of Ti could have performed as a refiner, contributing to the reduction of γ_2 phase (53.95%) and for the formation of two titanium phases: $CuNi_2Ti$ (41.65%) and $AlCu_2Ti$ (4.4%). The XRD pattern for the 0.7%Ti exhibited a benefic influence of the titanium content added in relation to reduction of brittle phase Cu_9Al_4 (38.70%). Furthermore, its addition contributed to phases $CuNi_2Ti$ (49.35%) and $AlCu_2Ti$ (6.31%) increase of quantity, and also, formed a typical martensitic structure, ordered by Cu_3Ti (5.6%) known as "X" phase as well [2].

3.3 SEM Analysis

The images obtained with SEM, in Figs. 2 and 3, favored the visualization of needle-like shape structure on each alloy, with and without Ti, typical of a martensitic structure. According to Otsuka and Wayman [11], these structures are characteristics of γ_2 phase, in which its presence on the alloy is confirmed through further XRD analyses. The sample CuAlNi, in Fig. 2a, showed thin grain boundaries and thin and long needles, identified by the red arrows, typical martensitic structure formed after heat treatment. The grains presented a polygonal morphology, with tendency equiaxial. The sample 0.5%Ti, in Fig. 2b, exhibited more visible and thick grain boundaries, when compared to the alloy without Ti, which could be related to the higher presence of γ_2 phase (95.02%), and also exhibited a small presence of "X" phase (4.98%) shown by the circled area in Fig. 2b.

In Figs. 3a and 3b, 0.6%Ti and 0.7%Ti reveled the "X" phase, identified by red arrows and circle. It is possible to notice that these samples, with 0.6% and 0.7% of Ti, presented a greater concentration of γ_2 phase and "X" phase, confirmed by the obtained XRD pattern.

3.4 Thermal Analyses—Phase Tranformation Temperature

Fig. 4 shows DSC results for the obtained samples. The reverse martensitic transformation (RMT) for CuAlNi occurred at a +20.46 °C (As) to +91.3 °C (Af) range. The DSC analysis presents a peak temperature of +62.31 °C (Ap), when the heat flow is maximal.

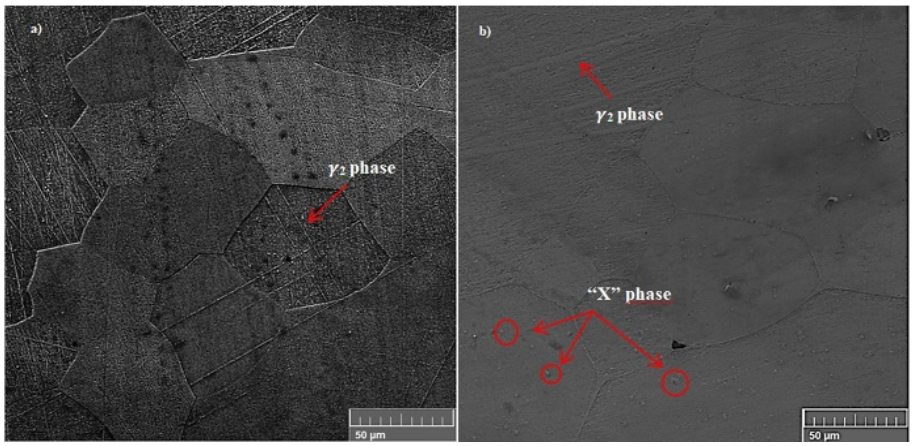

Fig. 2 SEM images of the alloys: (a) CuAlNi and (b) 0.5%Ti.

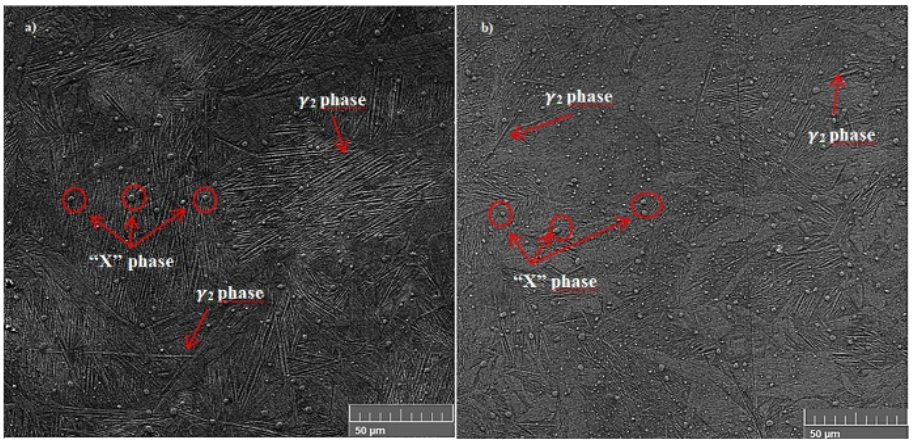

Fig. 3 SEM images of the alloys: (a) 0.6%Ti and (b) 0.7%Ti.

At cooling, the direct RMT occurs at a +131.15 °C (Ms) to +44.7 °C (Mf) range and peak temperature at +98.18 °C (Mp), associated with the exothermic process with 2.23 J/g enthalpy (Δh_M). The thermal hysteresis amplitude measurement was determined by the difference between critical peak temperatures and equal to 35.88 °C. The RMT of sample 0.5%Ti happens from +29.56 °C (As) to +102.80 °C (Af), through the endothermic process with phase transformation enthalpy of 1.9 J/g (Δh_A). The peak temperature registered was +91.53 °C (Ap).

At cooling, the direct RTM happens from +140.98 °C (Ms) to +87.00 °C (Mf), associated with the exothermic process with an enthalpy of 2.05 J/g (Δh_M) and a peak temperature of +123.80 °C (Mp). The thermal hysteresis was 32.27 °C. For sample 0.6%Ti, RMT occurs from +20.49 °C (As) to +97.8 °C (Af), in an endothermic process with a phase transformation enthalpy of 2.14 J/g (Δh_A). The recorded peak temperature was +86.7 °C (Ap). At cooling, the direct RMT occurs at a +130.08 °C (Ms) to +59.3 °C (Mf) range and peak temperature at 116.8 °C (Mp), associated with the exothermic process with a 2.2 J/g enthalpy (Δh_M). The hysteresis calculated was approximately 30.13 °C. The RMT of sample 0.7%Ti happens from +20.42 °C (As) to +82.8 °C (Af), through the endothermic process with phase transformation enthalpy of 2.1 J/g (Δh_A). The peak temperature recorded was +67.55 °C (Ap). At cooling, the direct RTM happens from +130.5 °C (Ms) to +44.55 °C (Mf), associated with the exothermic process with an enthalpy of 2.3 J/g (Δh_M) and a peak temperature of 99.4 °C (Mp). The thermal hysteresis was 31.86 °C.

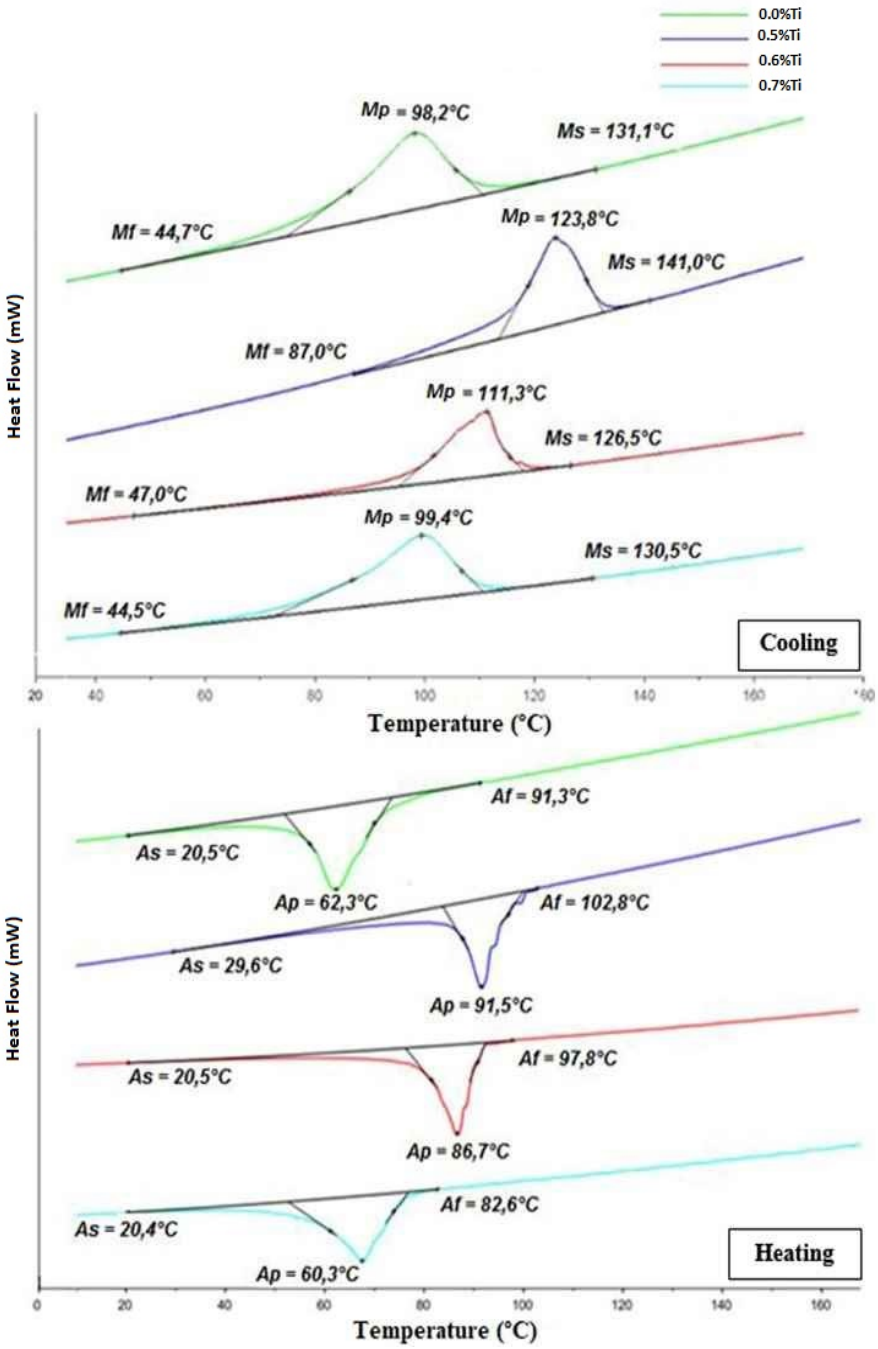

Fig. 4 DSC curves of samples: CuAlNi, 0.5%Ti, 0.6%Ti and 0.7%Ti.

Table 2 summarizes the critical temperatures of thermal events obtained for each sample DSC analyzed. The high value of M_s for 0.5%Ti could be related to the high percentage of γ_2 phase of chemical composition Cu_9Al_4. This phase has capability of increasing phase transformation temperatures [12]. The transformation temperature decreases with the increase of Al. With a 14 wt.% Al, the M_{Ps} is around environment temperature [13].

Probably, the low values for enthalpy and low thermal hysteresis variations among the samples were affected by the refinement mechanism due to the rapid solidification process. According to the comparative graph shown in Fig. 5, the enthalpy values and thermal

Table 2 Temperatures of thermal events analyzed by DSC.

CT (°C)	0.0%Ti	0.5%Ti	0.6%Ti	0.7%Ti
Ms	131.10	141.00	126.50	130.50
Mf	44.70	87.00	47.00	44.50
Mp	98.20	123.80	111.30	99.40
As	20.50	29.60	20.50	20.40
Af	91.30	102.80	97.80	82.60
Ap	62.30	91.50	86.70	60.30
Hysteresis	35.87	32.27	30.13	31.86
Δh_A (J/g)	2.07	1.90	2.14	2.10
Δh_M (J/g)	2.23	2.05	2.20	2.30

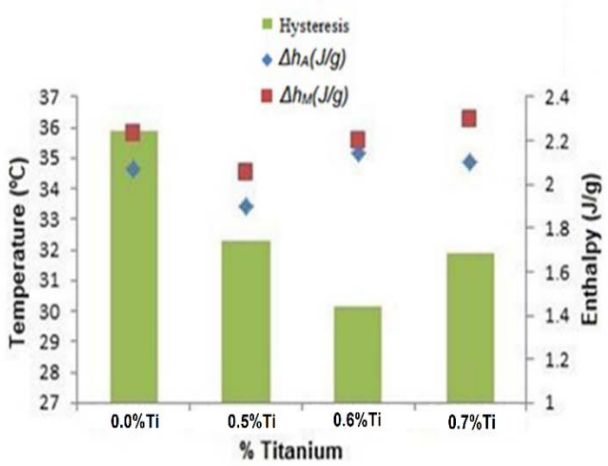

Fig. 5 Graph comparing phase transformation temperatures and enthalpies of the alloy.

hysteresis presented small variations between the alloy without Ti and the samples with different contents of Ti.

The enthalpies levels shown by the SMAs are relatively low, ranging from 1.9 J/g and 2.3 J/g. These values are consistent with the ones found in literature. And it was lower once comparing to 5.3 J/g obtained by Lee and Wayman [14]. Enthalpy could depend on the precipitates density, which are responsible for the grain growth. The low energy level involved in the phase transformation is linked to the microstructure refinement due to the rapid solidification process that reduces the crystalline lattice imperfections. However, a high hysteresis level in relation to the literature was observed. For example, a low hysteresis level is appreciable for sensor applications. For applications with a necessity of a shape recovery in large scale with sufficient force, for instance tube coupling, the transformation β_2 - β'_{19} (including β_2 - R) is useful. In this case, a high hysteresis value is required [11].

3.5 GS

Fig. 6 shows GS measurements for each obtained allow. The positive effect that the increase of titanium addition has on the Cu-14Al-4Ni SMA, rapidly solidified and submitted to betatization and quenching, in relation to GS reduction can be verified.

The GS reduction implies enhanced mechanical properties due to a reduction of brittleness. Rapid solidification rate tends to reduce the M_s [15]. A decrease of M_s is followed by a GS lowering and the increase of titanium content. Titanium addition causes GS decrease, in Table 3, because the titanium rich precipitates presences inhibit grain growth during betatization. Adding titanium implicates a martensitic transformation temperature reduction with an increase of solidification rate [14].

The GS decrease in function of the increase of titanium percentages can be justified by a Ti refinement

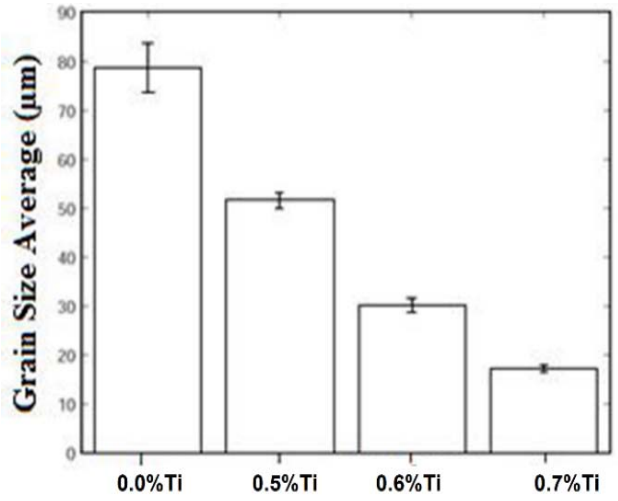

Fig. 6 Absolute GS measured by SEM, in µm.

Table 3 Average GS.

GS measurements	
Alloys	MEV (µm)
0.0%Ti	79.00 ± 5.0
0.5%Ti	48.00 ± 2.0
0.6%Ti	28.00 ± 1.0
0.7%Ti	16.00 ± 0.5

in the grain matrix. Titanium reduces diffusion rate of constituent atoms, resulting in grain refinement after casting. Therefore, titanium additions have an effective influence on the phase transformation behavior by the formation of new phases on the microstructure, Ti rich, which controls grain growth.

4. Conclusions

According to the analyses developed on this research, it was possible to verify and confirm the influence of different titanium contents on the martensitic transformation temperature of a Cu-14Al-4Ni SMA. The results obtained are summarized as following:

(1) The alloys presented a low enthalpy level, low start martensitic transformation temperatures (M_s), and hysteresis, which are followed by GS reduction (up to 80%) and the increase of titanium concentration;

(2) It is probable that the higher martensitic transformation temperatures presented for sample 0.5%Ti are related to the high Cu_9Al_4 phase percentages of 95.02%;

(3) However, the lower temperatures can be associated to the presence of titanium rich phases ($CuNi_2Ti$, $CuNi_2Ti$, Cu_3Ti and $AlCu_2Ti$), also known as "X" phase, and the rapid solidification process;

(4) The slight thermal hysteresis increase of 0.7%Ti, comparing to 0.6%Ti, could be a result of the Cu_3Ti phase presence;

(5) A reduction of the heat flow, which is necessary for the phase transformation, was noticed.

Acknowledgments

The authors would like to thank the Federal Institute of Science and Technology of Bahia, the University of São Paulo, the University of Brasilia and the PRPGI for all the support to carry out this research.

References

[1] Otsuka, K., and Wayman, C. M. 1999. "Characteristics of Shape Memory Alloys." In *Shape Memory Materials*, pp. 149-83.

[2] Saud, S. N., Hamzah, E., Abubakar, T., Ibrahim, M. K., and Bahador, A. 2005. "Effect of a Fourth Alloying Element on the Microstructure and Mechanical Properties of Cu-Al-Ni Shape Memory Alloys." *Journal of Materials Research* 30 (14): 2258-69.

[3] Font, J., Cesari, E., Muntasell, J., and Pons, J. 2003. "Thermomechanical Cycling in Cu-Al-Ni Based Melt-Spun Shape Memory Ribbons." *Materials Science and Engineering* 354: 207-11.

[4] Seguí, C., Pons, J., Cesari, E., Muntasell, J., and Font, J. 1999. "Characterization of a Hot-Rolled Cu-Al-Ni-Ti Shape Memory Alloy." *Materials Science and Engineering* 273-275: 625-9.

[5] Jones, H. 2001. "A Perspective on the Development of Rapid Solidification and Nanoequilibrium Processing and Its Future." *Materials Science and Engineering* 304-306: 11-9.

[6] ASTM E-112. 1996. *Standard Test Method for Average Grain Size*.

[7] Araki, Y., Endo, T., Omori, T., Sutou, Y., Koetaka, Y., Kainuma, R., and Ishida, K. 2011. "Potential of Superelastic Cu-Al-Mn Alloy Bars for Seismic Applications." *Earthquake Eng. Struct.* 40: 107-15.

[8] Gojic, M., Vrsalovic, L., Kozuh, S., Kneissl, A., Anzel, I., Gudic, S., Kosec, B., and Kliškic, M. 2011. "Electrochemical and Microstructural Study of Cu-Al-Ni Shape Memory Alloy." *J. Alloys Comp.* 2011: 9782-90.

[9] Lima, P. C. 2018. "Estudo do efeito da adição de titânio no tamanho de grão, nas temperaturas de transformação de fase e no módulo elástico da liga Cu-14Al-4Ni com efeito memória de forma obtida por fusão a arco e solidificação rápida a vácuo." Ph.D. thesis, Departamento de Engenharia Mecânica, Faculdade de Tecnologia, Universidade de Brasília - UnB. Brazil.

[10] Lojen, G., Anzel, I., Keneissl, A., Krizman, A., Unterweger, E., Kosec, B., and Bizjak, M. 2013. "Microstructure of Rapidly Solidified Cu-Al-Ni Shape Memory Alloy Ribbons." *Journal of Materials Processing Technology* 62: 220-2.

[11] Otsuka, K., and Wayman, C. M. 1999. "Characteristics of Shape Memory Alloys." In *Shape Memory Materials.* Cambridge: Cambridge University Press, 149-83.

[12] Rodriguez, P., and Guenin, G. 1990. "Thermal Ageing Behaviour and Origin of a Cu-Al-Ni." *Materials Science and Engineering* 129: 273-7.

[13] Lojen, G., Anzel, I., Keneissl, A., Krizman, A., Unterweger, E., Kosec, B., and Bizjak, M. 2005. "Microstructure of Rapidly Solidified Cu-Al-Ni Shape Memory Alloy Ribbons." *Journal of Materials Processing Technology* 162-163: 220-9.

[14] Lee, J. S., and Wayman, C. M. 1986. "Grain Refinement of a Cu-Al-Ni Shape Memory Alloy by Ti and Zr Additions." *Transactions of the Japan Institute of Metals* 27 (8): 584-91.

[15] Dutkiewicz, J., Czeppe, T., and Morgiel, J. 1999. "Effect of Titanium on Structure and Martensic Transformation in Rapidly Solidified Cu-Al-Ni-Mn-Ti Alloys." *Materials Science and Engineering* 273: 703-7.